Bulg. J. Phys. **44** (2017) 362–371

Global Correlations for Low-Lying Collective 2⁺ States

S. Pittel[1], **Z.Z. Qin**[2], **Y. Lei**[3], **R. Bijker**[4]

[1]Bartol Research Institute and Department of Physics and Astronomy, University of Delaware, Newark, Delaware 19716, USA

[2]School of Science, Southwest University of Science and Technology, Mianyang 621900, China

[3]Key laboratory of Neutron Physics, Institute of Nuclear Physics and Chemistry, China Academy of Engineering Physics, Mianyang 621900, China

[4]Instituto de Ciencias Nucleares, Universidad Nacional Autonoma de Mexico, A.P. 70-543, 04510 Mexico, D.F., Mexico

Received *23 October 2017*

Abstract. We show that both the triaxial rotor model and the anharmonic vibrator model with phonon mixing exhibit a global correlation between the quadrupole moments of the two lowest 2^+ states in collective nuclei, which had previously been observed in experimental data across the periodic table. We then derive other electromagnetic properties for these two models of nuclear structure and compare them with experimental data. We find that both robustly describe the data over the region of nuclei for which the models are applicable, including many that they have in common. We then show that there seems to exist a robust orthogonal transformation between these two models for realistic nuclear systems, suggesting that these two seemingly diverse descriptions of quadrupole collective phenomena seem to act in a similar model space and may therefore have a common origin.

PACS codes: 21.10.-k,21.10.Ky

1 Introduction

A large range of nuclei across the periodic table exhibit quadrupole collectivity. This includes nuclei that exhibit rotational, vibrational, triaxial and gamma-unstable features. Though these nuclei have a wide variety of different behaviors, there nevertheless appear some properties that are common to all. Here we focus on a feature reported recently in an experimental survey by Allmond [1], in which he showed that for a wide range of nuclei with $R = E(4_1^+)/E(2_1^+)$ values ranging from near the vibrational limit ($R = 2$) to near the rotational limit ($R = 3.33$) the quadrupole moments of the lowest 2^+ states, where both are measured, usually satisfy the property that $Q(2_1^+) \sim -Q(2_2^+)$. Allmond noted that this feature is reproduced theoretically for most nuclei by the IBM-1.

Here, we discuss two phenomenological models of nuclear structure that analytically reproduce this quadrupole moment correlation, the Triaxial Rotor Model (TRM) [2] and the Anharmonic Vibrator Model (AVM) [3–5] with phonon configuration mixing. As we will show, both not only incorporate the above correlation analytically but also do an excellent job of reproducing collective properties of low-lying quadrupole states across the periodic table.

The outline of the presentation is as follows. Following a brief review in Section 2 of the key elements of the two models and a demonstration that both satisfy the quadrupole moment correlation analytically, we show in Section 3 that both are able to successfully reproduce both spectroscopic and electromagnetic data, especially for 2^+ states, across the periodic table. In Section 4, we then discuss the possible relationship between these two apparently distinct collective models of nuclear structure by analyzing the orthogonal transformation that connects their bases for 2^+ states. Finally in Section 5, we show that the quadrupole moment correlation is fairly well reproduced in the IBM-2 model, suggesting that it may provide a natural framework for further investigation of the relationship between these models of quadrupole collective motion. Further details on the work described herein can be found in Refs. [6], [7].

2 Two Phenomenological Models of Nuclear Collective Motion

2.1 The TRM

The Triaxial Rotor Model (TRM) is a phenomenological model of nuclear structure. It contains a total of five parameters and has been used extensively to describe experimental data on E2 collectivity across several regions of the periodic table [8–11]. Here we briefly summarize the key components of its formalism as needed for our investigation.

The Hamiltonian matrices for 2^+ and 4^+ states in the model are given by

$$H_{\mathrm{TRM}}^{2^+} = \begin{pmatrix} 6A & 4\sqrt{3}G \\ 4\sqrt{3}G & 6A+4F \end{pmatrix} ,$$
$$H_{\mathrm{TRM}}^{4^+} = \begin{pmatrix} 20A & 12\sqrt{5}G & 0 \\ 12\sqrt{5}G & 20A+4F & 4\sqrt{7}G \\ 0 & 4\sqrt{7}G & 20A+16F \end{pmatrix} , \tag{1}$$

with A, G and F being Hamiltonian parameters related to the three components of the inertia tensor.

The lowest 2^+ states of the model are orthogonal combinations of the $K = 0$

and $K = 2$ basis configurations,

$$|2_1^+\rangle = \cos\Gamma|K=0\rangle - \sin\Gamma|K=2\rangle \ ,$$
$$|2_2^+\rangle = \sin\Gamma|K=0\rangle + \cos\Gamma|K=2\rangle \ . \tag{2}$$

Here K is the projection of the angular momentum with respect to the intrinsic coordinate system, and $\tan 2\Gamma = 2\sqrt{3}G/F$ defines the mixing of these basis configurations.

The E2 properties of the lowest 2^+ states can be expressed compactly as

$$\begin{aligned}
\mathrm{B(E2,}2_1^+ \to 0_1^+) &= \frac{Q_0^2}{16\pi}\cos^2(\gamma+\Gamma) \ ,\\
\mathrm{B(E2,}2_2^+ \to 0_1^+) &= \frac{Q_0^2}{16\pi}\sin^2(\gamma+\Gamma) \ ,\\
\mathrm{B(E2,}2_2^+ \to 2_1^+) &= \frac{5Q_0^2}{56\pi}\sin^2(\gamma-2\Gamma) \ ,\\
Q(2_1^+) &= -\frac{2}{7}\,Q_0\cos(\gamma-2\Gamma) = -Q(2_2^+) \ .
\end{aligned} \tag{3}$$

Here Q_0 is the static quadrupole moment, and γ is a parameter related to the nuclear quadrupole deformation. Note from the last line of eq.(3) that a $Q(2_1^+) = -Q(2_2^+)$ correlation is unconditionally conserved in the TRM.

2.2 The AHV

In the AHV description of nuclei [4] with phonon configuration mixing, the model space of 2^+ states is constructed from one- and two-phonon excitations of the phonon vacuum $|0\rangle$ (the 0^+ ground state of the system), denoted as $|1\rangle$ and $|2\rangle$, respectively.

In this model space, the Hamiltonian matrix for 2^+ states can be written as

$$H_{\mathrm{AHV}}^{2^+} = \begin{pmatrix} \hbar\omega & \lambda \\ \lambda & 2\hbar\omega \end{pmatrix} \ , \tag{4}$$

where $\hbar\omega$ is the phonon energy and λ defines the mixing between one- and two-phonon configurations. Denoting the one- and two-phonon basis states as $|1\rangle$ and $|2\rangle$, respectively, the eigenstates of this Hamiltonian are given by

$$|2_1^+\rangle = a_1|1\rangle + a_2|2\rangle \ ,$$
$$|2_2^+\rangle = -a_2|1\rangle + a_1|2\rangle \ , \tag{5}$$

where $a_1^2 + a_2^2 = 1$.

The E2 operator in the model, $\hat{Q} = \chi(b^\dagger + \tilde{b})$, is the sum of phonon creation and annihilation operators multiplied by a free parameter χ. Quadrupole properties can be summarized as

$$
\begin{aligned}
\mathrm{B(E2,}2_1^+ \to 0_1^+) &= \frac{\chi^2 a_1^2}{5} \langle 0||\tilde{b}||1\rangle^2 \ , \\
\mathrm{B(E2,}2_2^+ \to 0_1^+) &= \frac{\chi^2 a_2^2}{5} \langle 0||\tilde{b}||1\rangle^2 \ , \\
\mathrm{B(E2,}2_2^+ \to 2_1^+) &= \frac{\chi^2 (a_1^2 - a_2^2)^2}{5} \langle 1||\tilde{b}||2\rangle^2 \ , \\
Q(2_1^+) = \frac{8\chi a_1 a_2}{5} & \sqrt{\frac{2\pi}{7}} \langle 1||\tilde{b}||2\rangle = -Q(2_2^+) \ . \qquad (6)
\end{aligned}
$$

Here too the desired quadrupole moment correlation emerges naturally, independent of the precise spectral behavior exhibited by the nucleus being described. We should emphasize, however, that this only arises when we ignore multi-phonon mixing.

3 Systematic Comparison with Data

3.1 Spectral properties

Diagonalization of Eq. (1) for given values of A, F and G provides excitation energies of 2_1^+, 2_2^+ and 4_1^+ states in the TRM approach. We refer to the 203 nuclei for which this approach yields a fit to the data in [13] as TRM-solvable nuclei and present in Figure 1 the $R = E(4_1^+)/E(2_1^+)$ distribution of these nuclei. The distribution spreads over the whole $R > 2$ region, indicating that the TRM can describe non-rotor-like spectra, while still maintaining the rotational

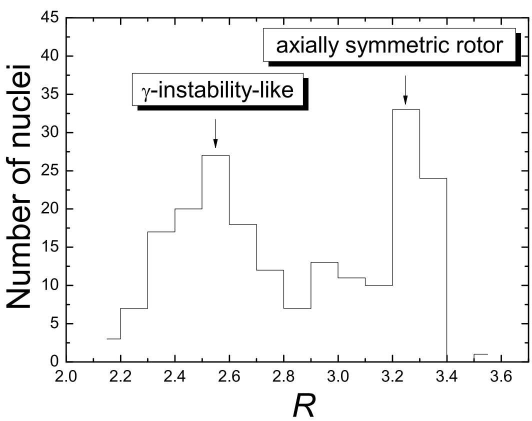

Figure 1. $R = E(4_1^+)/E(2_1^+)$ distribution of the 203 TRM-solvable nuclei in the ENSDF. Peaks for γ-instability ($R \simeq 5/2$) and an axially-symmetric rotor ($R \simeq 10/3$) are highlighted.

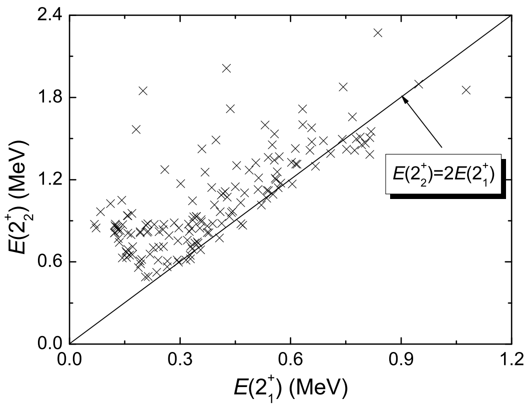

Figure 2. Experimental $E(2^+_2)$ versus $E(2^+_1)$ for the 177 nuclei with $R = 2.05 \sim 3.15$ in the ENSDF. The $E(2^+_2) = 2E(2^+_1)$ line is highlighted.

quadrupole moment correlation. We also note that there are two peaks in the distribution, one near $R = 10/3$ peak corresponding to axially-symmetric rotational nuclei and one near $R = 5/2$ corresponding to γ-unstable nuclei (*i.e.* near the $SO(6)$ limit of the IBM [14]).

The spectral structure of nuclei within the AHV approach is simpler than for the TRM. Since the 2^+_1 and 2^+_2 states arise from mixing one- and two-phonon configurations, the lowest 2^+ state must lie below the one-phonon excitation energy, $\hbar\omega$, whereas the second 2^+ state must be above $2\hbar\omega$. Figure 2 shows all available experimental data on nuclei with $E(2^+_2)$ versus $E(2^+_1)$ in the range $R = 2.05 \sim 3.15$. This includes 177 nuclei in the ENSDF. Clearly most such nuclei sit above the $E(2^+_2) = 2E(2^+_1)$ line, suggesting that the ensemble of $R = 2.05 \sim 3.15$ nuclei is indeed an appropriate sample of AHV-applicable nuclei, in agreement with the classification of Casten *et al.* [15].

3.2 E2 collectivity

We now focus on correlations between E2 transition rates and the quadrupole moments of the two lowest 2^+ states in the two models. From earlier formulae presented for the TRM (3), we can obtain the following *approximate* relation between the BE2 values and quadrupole moments of 2^+ states:

$$\begin{aligned}\mathrm{B(E2,}2^+_1 \to 0^+_1) + \mathrm{B(E2,}2^+_2 \to 0^+_1) \simeq 0.7\,\mathrm{B(E2,}2^+_2 \to 2^+_1) \\ + 0.244\, Q^2(2^+_1)\,. \end{aligned} \tag{7}$$

For the AHV (6), we can derive an analogous approximate formula:

$$\begin{aligned}\mathrm{B(E2,}\, 2^+_1 \to 0^+_1) + \mathrm{B(E2,}\, 2^+_2 \to 0^+_1) \simeq 0.5\,\mathrm{B(E2,}\, 2^+_2 \to 2^+_1) \\ + 0.174\, Q^2(2^+_1)\,. \end{aligned} \tag{8}$$

Both are in the general form of Kumar-Cline sum rules, which takes the form

$$\mathrm{B(E2},\, 2_1^+ \to 0_1^+) + \mathrm{B(E2},\, 2_2^+ \to 0_1^+) = c_1\, \mathrm{B(E2},\, 2_2^+ \to 2_1^+) + c_2\, Q^2(2_1^+)\,, \tag{9}$$

with c_1 and c_2 being free variables.

We perform a multiple linear fitting of (9) to all available experimental data from the ENSDF using c_1 and c_2 as fitting parameters. A total of 78 nuclei are considered in the fit of the left side to the right side, with the correlation coefficient of $r = 0.980$ that emerges being very close to 1. This confirms that B(E2) values between ground states and low-lying 2^+ states are highly correlated with $Q(2_1^+)$ in the ENSDF. The best-fit results are $c_1 = 0.479$ and $c_2 = 0.188$, substantially closer to the AHV coefficients.

Using Eqs. (7) for the TRM and (8) for the AHV, we estimate the magnitudes of the quadrupole moments $Q(2_1^+)$ from the experimentally available B(E2) values. In Figure 3, we plot the $|Q(2_1^+)|$ values that emerge in comparison with the associated experimental values. For both models, the data points of both models scatter reasonably closely around the diagonal line, confirming that both models provide meaningful global descriptions of low-lying E2 collectivity.

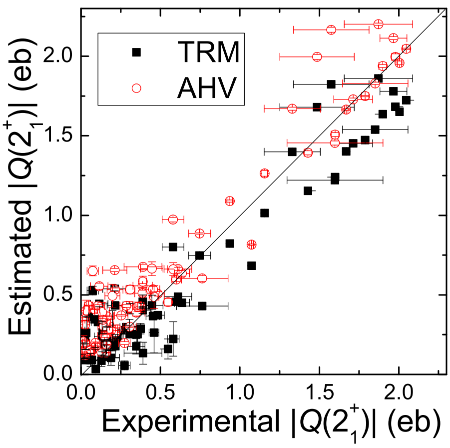

Figure 3. (color online) Plot of the estimated $|Q(2_1^+)|$ values based on the use of experimental B(E2) values according to Eqs. (7) and (8), against the experimental data, for the 78 nuclei with available data in the ENSDF. The diagonal line is a measure of the quality of the estimates.

4 What Next?

We have seen that both the TRM and the AHV provide fairly robust descriptions of excitation energies and E2 properties, especially for collective 2^+ states. Furthermore, in both models, the 2^+ states are described in terms of a two-state basis. Since both models describe the same set of properties in terms of matrices of the same dimension, we can find an orthogonal transformation between those matrices for each such nucleus,

$$U = \begin{bmatrix} \cos\theta & \sin\theta \\ -\sin\theta & \cos\theta \end{bmatrix}, \tag{10}$$

such that

$$H^{2+}_{\mathrm{TRM}} = U H^{2+}_{\mathrm{AHV}} U^{\mathrm{T}}. \tag{11}$$

We would now like to see whether there is an intrinsic connection between the TRM and the AHV models for realistic nuclei. That would be the case if there were a *unique* orthogonal transformation that relates the two bases, namely the K basis of the TRM and the phonon basis of the AHV, *viz.*

$$\begin{bmatrix} K=0 \\ K=2 \end{bmatrix} = U \begin{bmatrix} |1\rangle \\ |2\rangle \end{bmatrix}. \tag{12}$$

To address this, we calculate the distribution of θ values. We do so in such a way as to remove any bias due to the fact that the θ value for a given nucleus should most likely be correlated with the R value for that same nucleus. Details on how this is done can be found in [6]. As noted there, that we can only get information on $|\theta|$, since θ and $-\theta$ define the same transformation.

The resulting distribution of $|\theta|$ values, denoted $P(|\theta|)$, is shown in Figure 4 for the 203 nuclei in the ENSDF that are TRM- *and* AHV-solvable. What we see is

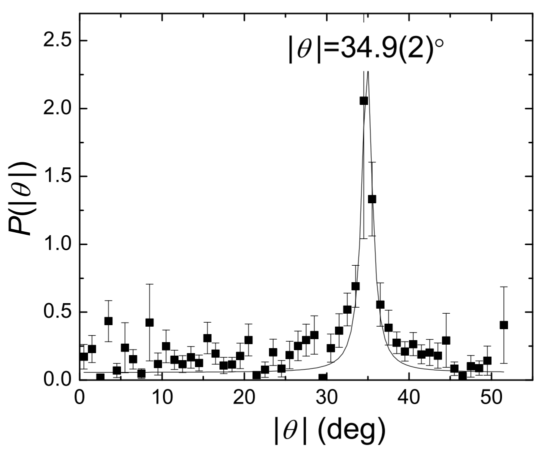

Figure 4. R-normalized $P(|\theta|)$ distribution (square points). The error bar represents the statistical error. The peak fit (solid line) has its center at $|\theta| = 34.9(2)^\circ$, as highlighted. This figure uses the same statistical ensemble as in Figure 1.

that there is a single dominant peak, centered near $|\theta| = 34.9°$, suggesting that the bases used in the two sets of analyses (for 2^+ states) do indeed to a good approximation seem be the same.

This raises the question of whether the underlying physics of quadrupole collective motion described by these two models may have a deeper origin, with the TRM and AHV descriptions contained within a richer model of quadrupole collectivity.

5 The Global Quadrupole Moment Correlation in the IBM

In his article in which the global quadrupole moment correlation was first discussed, Allmond [1] noted that the correlation seems to be reproduced fairly generally in the IBM-1 within a consistent-Q framework. No numerical results were shown, however. Here we briefly expand on those considerations by presenting numerical results under a variety of different scenarios, but now using the IBM-2 with its somewhat broader range of collective behaviors.

In Table 1, we show results for the ratio of quadrupole moements between the lowest two 2^+ states at or near several symmetry limits of the model. The results denoted SU(3), SU(5) and SU(3)* refer to precise symmetry limits. In contrast to the first two, the SU(3)* results, which refer to a pure triaxial rotor [16], *require* a full IBM-2 treatment. In the exact O(6) limit, for which $\chi_\pi = \chi_\nu = 0$, the quadrupole moments are identically zero, and thus we considered a slight breaking of the symmetry (denoted by δ) by including a small amount of either SU(3) mixing or SU(3)* mixing, implemented by setting $\chi_\pi = \chi_\nu = 0.10$ (for SU(3) mixing) and $\chi_\pi = 0.10,\ \chi_\nu = -0.10$ (for SU(3)* mixing).

Table 1. Selected results for the ratio of quadrupole moments of the lowest two 2^+ states in the IBM-2 under a variety of conditions. All results are for $N_\pi = 3$ and $N_\nu = 5$ bosons.

	$SU(3)$	$SU^*(3)$	$U(5)$	$SO(6)+\delta(SU(3))$	$SO(6)+\delta(SU^*(3))$
$Q(2_1^+)/Q(2_2^+)$	-1.20	-1.00	-2.28	-1.04	-1.04

In Table 2, we explore the transition between vibrational and deformed nuclei, via a parametrized IBM-2 Hamiltonian

$$H = (1-\xi)(n_{d_\pi} + n_{d_\nu}) - \xi\,\frac{N_\pi + N_\nu}{N_\pi N_\nu}\,Q_\pi \cdot Q_\nu\ , \tag{13}$$

with ξ varying from 0 to 1. When $\xi = 1$, this Hamiltonian produces rotational motion, which smoothly evolves to vibrational motion as ξ is decreased to 0. At $\xi \approx 0.2$, a shape phase transition takes place and the spectrum involves significant level crossings. At that point we therefore show the ratio of $Q(2_1^+)/Q(2_4^+)$, to reflect the 2^+ states with the same structure as prior to the transition. As is

Table 2. Results for the ratio of quadrupole moments of the lowest two 2^+ states in the IBM-2 across the transition from vibrational to rotational nuclei, as produced by the Hamiltonian in Eq. 13. All results are for $N_\pi = 3$ and $N_\nu = 5$ bosons. At $\xi = 0.2$, the results denoted by a * refer to $Q(2_1^+)/Q(2_4^+)$.

ξ	$Q(2_1^+)/Q(2_2^+)$	ξ	$Q(2_1^+)/Q(2_2^+)$	ξ	$Q(2_1^+)/Q(2_2^+)$
0.0	-2.33	0.4	-1.27	0.8	-1.20
0.1	-2.30	0.5	-1.24	0.9	-1.21
0.2^*	-2.31	0.6	-1.23	1.0	-1.21
0.3	-1.46	0.7	-1.25		

clear from the table, below the shape transition the ratio of quadrupole moments is roughly $-7/3$, typical of a vibrational nucleus. Above the transition point, the ratio rapidly falls to a typical rotational value.

All results are compatible with the general features found by Allmond, namely that $Q(2_1^+)$ and $Q(2_2^+)$ have opposite signs and roughly the same magnitudes (within a factor of roughly 2). However, as also pointed out by Allmond, in rotational nuclei it is critical that the second 2^+ state not be part of a β band for this to emerge.

6 Summary

We have discussed two phenomenological models of nuclear structure, the TRM and the AHV, both of which analytically satisfy the property $Q(2_1^+) = -Q(2_2^+)$ that has been found globally for nuclei exhibiting quadrupole collectivity. We have shown that both models can describe systematic correlations between excitation energies and E2 collectivity, especially for the lowest two 2^+ states, across a wide range of the periodic table, and that they produce good overall agreement with the associated experimental data. We also showed that the TRM and AHV Hamiltonian matrices for 2^+ states can be connected by an orthogonal transformation that is roughly the same for most nuclei. This suggests that the TRM and AHV, though apparently very different models of nuclear collectivity, seem to have a common model space for realistic nuclear systems, and thus are perhaps just two aspects of a more general model of quadrupole collective behavior. The Neutron-Proton Interacting Boson Model (IBM-2) seems an appropriate framework in which to explore this further.

Acknowledgments

This work was supported in part by the National Natural Science Foundation of China under Grant No. 11647059 and 11305151, the Research Fund for the Doctoral Program of the Southwest University of Science and Technology under Grant No. 14zx7102, and by PAPIIT-DGAPA, UNAM under Grant No. IN109017. SP wishes to acknowledge the Bulgarian fund under contract No. DFNI-E02/6 for their support of his participation in SDANCA17.

References

[1] J.M. Allmond (2013) *Phys. Rev. C* **88** 041307.
[2] A.S. Davydov and G.F. Filippov (1958) *Nucl. Phys.* **8** 237.
[3] F.K. McGowan, R.L. Robinson, P.H. Stelson, and J.L.C. Ford Jr. (1965) *Nucl. Phys.* **66** 97.
[4] T. Tamura and T. Udagawa (1966) *Phys. Rev.* **150** 783.
[5] D.R. Bes and G.G. Dussel (1969) *Nucl. Phys. A* **135** 1.
[6] Z.Z. Qin, Y. Lei, and S. Pittel (2016) *Phys. Rev. C* **94** 024301.
[7] Z.Z. Qin, Y. Lei, S. Pittel, and R. Bijker (2017) *J. Phys. Conf. Ser.* **876** 012019.
[8] J.M. Allmond, R. Zaballa, A.M. Oros-Peusquens, W.D. Kulp, and J.L. Wood (2008) *Phys. Rev.* C **78** 014302.
[9] J.M. Allmond, J.L. Wood, and W.D. Kulp (2010) *Phys. Rev. C* **81** 051305.
[10] W.D. Kulp, *et al.* (2006) *Phys. Rev. C* **73** 014308.
[11] A.D. Ayangeakaa, *et al.* (2016) *Phys. Lett. B* **754** 254.
[12] J.L. Wood, A-M. Oros-Peusquens, R. Zaballa, J.M. Allmond, and W.D. Kulp (2004) *Phys. Rev. C* **70** 024308.
[13] Evaluated Nuclear Structure Data File Retrieval, http://www.nndc.bnl.gov/ensdf/.
[14] F. Iachello and A. Arima (1987) "*The Interacting Boson Model*" (Cambridge University, Cambridge, UK).
[15] R.F. Casten, N.V. Zamfir, and D.S. Brenner (1993) *Phys. Rev. Lett*. **71** 227.
[16] A.E.L. Dieperink and R. Bijker (1982) *Phys. Lett. B* **116** 77.